ISSN 0853-2982 eISSN 2549-2659

JURNAL TEKNIK SIPIL

Jurnal Teoretis dan Terapan Bidang Rekayasa Sipil

Engineering Characterization of Earthquake Ground Motions Based on Composite-intensity Index Spectrum

Sindur P. Mangkoesoebroto(*)

Civil Engineering Department, Institute of Technology Bandung, Jalan Ganesha 10, Bandung 40132, Indonesia.
Email: sindurpm@gmail.com; phone: +62 22 250 4669

Niakku I. Maggang

Centre for Industrial Research, Institute of Technology Bandung, Jalan Ganesha 10, Bandung 40132, Indonesia.

Abstract

This study proposed an alternative method to earthquake ground motion characterization based on composite-intensity index spectrum. It is a combination of spectral acceleration ($S_a(T)$), duration (D_{05-95}) and peak ground velocity (PGV). The spectrum, considering the effect of three-component motions, was firstly introduced in the paper. It was established based on thirty-one three-component strong earthquake records that were collected worldwide. The index was further related to the modified Mercalli intensity scales to assign its damage potentials. The method revealed more meaningful interpretations of earthquake ground motion characterization than other procedures.

Keywords: Earthquake motion characterization, three components, composite-intensity index, acceleration spectrum, duration, peak ground velocity, MMI.

Abstrak

Studi ini mengusulkan metode alternatif terkait karakterisasi gelombang gempa berdasarkan spektrum indeks intensitas komposit. Indeks ini adalah gabungan dari spektra percepatan ($S_a(T)$), durasi (D_{05-95}) dan kecepatan puncak permukaan (PGV). Spektrum indeks intensitas komposit, dengan tinjauan gelombang gempa tiga-komponen, adalah yang diusulkan pertama kali dalam makalah ini. Metode ini dikembangkan berdasarkan tiga-puluh satu gelombang gempa tiga-komponen yang tersebar di dunia. Indeks tersebut selanjutnya diikatkan dengan skala intensitas Mercalli termodifikasi untuk menunjukkan potensi kerusakannya. Hasil yang diperoleh menunjukkan bahwa karakterisasi gelombang kuat dapat dilakukan berdasar indeks intensitas komposit lebih baik daripada metode lain yang tersedia.

Kata kunci: Karakterisasi gelombang gempa, tiga komponen, indeks intensitas komposit, spektrum percepatan, durasi, kecepatan puncak, permukaan, skala MMI.

1. Introduction

Earthquake ground motion engineering characterization had been a long-standing issue. It aimed at predicting the damage potentials of the emerging strong ground motions through few parameters computed based on the recorded time series, e.g., accelerations. In the characterization process, intensity measures (IMs) were commonly established consisting of one or more parameters (e.g., peak amplitudes and/or spectral values) formulated in certain relations. The IMs were expected to have a correlation with damage states induced by earthquake events. The damage states could be in the form of damage measures (DMs), e.g., inter-story drift angle, hysteretic energy dissipation, plastic collapse mechanism; or in terms of macroseismic intensity scales, e.g., modified Mercalli intensity scales. In the former, models of structures were investigated via computations and/or experiments to find correlations between the defined IMs and DMs. The IMs should meet the conditions of efficiency and sufficiency (Luco and Cornell, 2007). Hence, in this case, the IMs had specific relations with the DMs for specific models being investigated. In the latter, the IMs were related to the macroseismic intensity scales via regression analyses based on earthquake ground motion records associated with the observed damage states in the vicinity of the recording stations (Wald *et. al.*, 1999, Garcia and Bernal, 2008). Unlike the damage states inferred from DMs as in the former scenario, the damage states inferred from macroseismic intensity scales reflected the aspects of building category/ quality, material, workmanship, construction date, etc. In line with the latter, the aim of the study was to propose an IM which was formulated in a systematic manner based on three-component of several earthquake ground motions. The IM would then be correlated with the Mercalli macroseismic intensity scales to assign its damage potentials. Subsequently,

*Corresponding Author

Diterima 8 Oktober 2021, Direvisi 31 Maret 2022, Diterima untuk dipublikasikan 25 April 2022

the IM could be used to predict the damage potentials of the emerging earthquake events.

Many ground motion intensity measures (IMs) were already proposed (e.g., Kramer and Mitchell, 2006, Zhang *et. al*., 2018). In most earthquake ground motion characterizations, the peak-amplitude, and spectral values as well as the durations were determined and analysed to assess the damaging potentials of the earthquake event. For instance, in the case of Chi-Chi earthquake 1999, Taiwan, Wu *et. al.* (2003) found that the peak ground velocity (PGV) was much better correlated to damage than with PGA. Similar conclusion was reported during the 2011 Tohoku earthquake (Wu *et. al.*, 2012) where the damage ratio was better correlated with PGV, the JMA macroseismic intensity, and the Housner spectrum intensity (see **Eq. (10)**), than with PGA. Further, Bommer and Alarcon (2006) pointed out that many found high correlation between earthquake damaging potentials with PGV. Bradley (2012) derived empirical relations between PGV and PGA, spectrum of pseudo-acceleration ($S_{pa}(T$=0.01-10 seconds, ζ=5%)), the acceleration spectrum intensity♠, and the Housner spectrum intensity. However, the contrary was reported by Bijukchhen *et. al.* (2017) after the devastating Gorkha 2015, Nepal, earthquake. Despite its high PGV of about 99 cm/sec, the damage, in general, was relatively lower than that previously anticipated. Hence, earthquake characterization based on PGV alone was inadequate. Further, Goto and Morikawa (2012) pointed out that some other earthquake parameters beside PGV and PGA needed to be accounted for after the Tohoku 2011, Japan, earthquake, supporting earlier views (Wu *et. al.*, 2012).

Massumi and Selkisari (2017) studied the correlation among IMs with damage indices for some different RC frames. While asserting that there was no single IM that could have a high correlation with damage, they showed that among the spectral parameters, velocity spectrum intensity♣ (VSI) had the maximum correlation with Park-Ang damage index. With a similar model, Kamal and Inel (2021) found that the Housner spectrum intensity had the strongest correlation with the building damage potentials among the investigated IMs. Sandeep and Prasad (2012) studied four earthquakes (i.e., Kobe 1995, Chalfant Valley 1995, Whittier Narrows 1987, and Chi-Chi 1999) and concluded that the velocity spectrum intensity showed stronger correlation with damage than with PGA, magnitude, and distance.

Elenas (2000) found a high correlation between Park-Ang damage index of reinforced concrete framed structure with the pseudo-acceleration spectrum and input energy at a lesser degree. Zhang *et. al.* (2018) proposed ground motion IM based on a combination of spectral acceleration values at some periods. Comparisons with some other IMs were explored and good consistency was produced. Perrault and Guéguen (2015), based on the California earthquakes, considered not only the effect of several spectral frequencies but also the combination of several earthquake parameters, to the total building story drifts as the DM. They concluded that the combination of four earthquake parameters, i.e., PGA, cumulative absolute velocity (CAV), S_d (T_1), and the mean of S_v, provided the least variations in the DM. Meanwhile, the use of the spectral accelerations in one direction or the average that of the two-direction as IMs was discussed in Baker and Cornell (2006).

Yahyaabadi and Tehranizadeh (2011) compared the velocity and displacement spectrum in relation to the DM of structures (i.e., the maximum inter-story drift angle), and found that, though they were comparable, the displacement spectrum yielded less variations. Their proposed IM was basically the combination of displacement spectrum at different periods of structures. The periods, also considering their lengthening effect due to structures' inelastic behaviour of the first (T_1) as well as higher modes (T_2), were employed to determine spectral displacements, which was further combined in a way to minimize its variability. (Katsanos *et. al.* (2014) asserted that period lengthening did occur in structures when subjected to earthquake ground motions especially in RC structures, and this needed to be considered in estimating damage potential based on spectral-related IMs.)

The effect of duration on structural damage has been of interest for a long time (Trifunac and Brady, 1975). At least about thirty definitions of the duration of ground motion records were studied by Bommer and Martinez -Pereira (1999). The need to consider strong motion duration in the mapped parameters was also emphasized in Bozorgnia and Campbell (2004). However, duration alone might be unable to reflect the damage potential of ground motions sufficiently, but its product with other seismic parameters, e.g., PGV, might better reflect it (Bommer and Alarcon, 2006, Fajfar *et. al.,* 1990). In another study, it was revealed that the significance of duration related to damage was open to debate depending on what DMs and the structural models used (Hancock and Bommer, 2006). However, in the case of the Wenchuan 2008 earthquake, China, the duration was very long and the human casualties, as well as infrastructure damages, were unprecedentedly high (Xie *et. al.,* 2012). In the case of concrete-faced rockfill dams, Xu, *et. al* (2018) observed that the crest displacements were strongly correlated with duration, but the face-slab damage index correlated with the PGA. That the duration was strongly correlated with the rocking demand of rigid structures was observed by Giouvanidis and Dimitrakopoulos (2018).

♠ The acceleration spectrum intensity was the integral of the $S_{pa}(T, z$=5%) over $0.1 \leq T$(sec) ≤ 0.5 (Von Thun *et. al.*, 1988).

♣ The velocity spectrum intensity (VSI) was the integral of $S_{pv}(T, z$=5%) over $0.1 \leq T$(sec) ≤ 2.5 (Von Thun *et. al.*, 1988). Indeed, this is the same as the Housner spectrum intensity (see Eq. (10)).

Diterima 8 Oktober 2021, Direvisi 31 Maret 2022, Diterima untuk dipublikasikan 25 April 2022

The list of these IMs can be extended to include more parameters (Kramer and Mitchell, 2006, Zhang *et. al.*, 2018). Some IMs, furthermore, could be estimated from others; for example, the modified Mercalli intensity could be assessed from PGA and PGV (Garcia and Bernal, 2008), and such as in the ShakeMaps (Wald *et. al.*, 1999), and subsequently verified by field observation. Despite its long list, presently, most ground motion characterizations were based on one component of the records, or two but separately, and none was performed based on three-component, albeit the vertical component together with the horizontal was found to be capable of causing more damage to structures (Ghobarah and Elnashai, 1998).

The above discussions showed that the earthquake characterization performed thus far were ambiguous and, at best, revealed only part of the phenomena of the seismic events (Kamal and Inel, 2021). This was because the IMs used were not systematically structured, and none considered the effect of three-component motions simultaneously. The IM proposed in this study was systematically structured and based on three-component motions and were correlated with the macroseismic intensity scales (MMI) to assign its damage potentials, and hence, it was expected to be a more realistic engineering characterization of ground motions.

2. Methodology

The study began with selecting some earthquake events. The number of the events is not restricted to any values, but statistical significance would be achieved for about thirty events or more. In Section 3 the ground motions were presented and discussed. For each earthquake event, some parameters based on three-component motions were evaluated. The parameters included the peak ground acceleration, velocity, displacement, etc. The number of parameters was immaterial, but parameters commonly adopted by other investigators were investigated herein. These parameters were quantified in Section 4 and there are about nineteen. The correlation coefficients among the parameters were computed considering all earthquake events, and the parameters were grouped based on these coefficients. Three parameters were fully correlated, leaving the remaining sixteen for further analyses. For illustration, at one second period, the spectral acceleration, $S_a(T=1)$, together with spectral velocity, $S_v(T=1)$, the spectral energy input, $E_{in}(T=1)$, and input power, $P_{in}(T=1)$, were in one group because any pair were correlated very strong (above 80 percent). In the group, one parameter was selected as the lead parameter, in this case, $S_a(T=1)$ was the lead parameter of the first group, because it showed the highest correlation, and was widely used in other studies. Other groups were investigated similarly with their own lead parameters. The groups are disjoint sets, and their members vary from one to four parameters. In total there were ten groups to represent all sixteen parameters with high correlation coefficients (above 80 percent). Out of sixteen parameters, however, the first three groups with the spectral acceleration ($S_a(T=1)$), significant duration ($D_{05\text{-}95}$) and peak ground velocity (PGV) as the lead parameters already represented ten parameters (four for $S_a(T=1)$, and each three for the other two) with high correlations (above 80 percent). Next, a diagonal matrix consisting of the lead parameters was constructed. The strength of the matrix was measured by its norm, which was used as the basis to define a composite-intensity index. The procedures were repeated for twenty-four periods so that a composite-intensity index spectrum could be created. The index was related to the Mercalli macroseismic intensity scales (MMI) to assign its damage potentials. Consequently, specific damage measures (e.g., drift, plastic collapse mechanism, hysteretic energy dissipation) were not required in this study.

The detailed procedure is described in the following steps.

1. Earthquake event collection: The earthquake data were compiled from public domain databases. The data should include events with varying Mercalli macroseismic intensity (MMI). For this purpose, events with intensities higher than VII MMI were considered. The number was so that statistical significance could be represented. A number more than thirty should suffice. They should be statistically independent.
2. Seismic parameters: Parameters computed based on three-component motions to characterize a seismic event should be defined, e.g., peak ground acceleration (PGA), velocity (PGV), displacement (PGD), pseudo-spectral acceleration, velocity, displacement ($S_{pa}(T)$, $S_{pv}(T)$, $S_d(T)$), etc. They could be as many as practicable. In this study about nineteen parameters were investigated.
3. Correlation coefficients: All seismic parameters were assumed lognormally distributed; hence, their common logarithm values were considered. Correlation coefficients among the lognormally seismic parameters covering all earthquake events were computed and identified. To avoid duplication, parameters with correlation coefficients of unity were screened out from further analyses.
4. Parameter grouping: Parameters were grouped based on their correlations. Each group was populated by parameters with correlations higher than 80% among them. The first group was the most populated; the last was the least. The groups were disjoint, when there were ties, the less populated group gave up its tied parameters.
5. Lead parameters: For each group, the lead parameter was selected based on the highest correlation in the group, or the most used in other studies.
6. Normalization of parameters: The seismic parameters have different units and values, so it is necessary to make them unitless and normalized to make them less likely to produce biases. The normalization process makes each parameter have a unit standard deviation, a mean value of κ and becomes an index. The value of κ is so chosen that no parameter has negative values for all earthquake events after normalization. This process does not alter the correlations among parameters.

Diterima 8 Oktober 2021, Direvisi 31 Maret 2022, Diterima untuk dipublikasikan 25 April 2022

7. Weight factors of the lead parameters: The total number of the groups was such that the total number of parameters was all covered. As illustration, at period of T=1 second, group 1 was populated by parameters 1,2,3 and 4 or g_1 ($\mathbf{p_1}$,p_2,p_3,p_4); similarly g_2($\mathbf{p_5}$,p_6,p_7), g_3($\mathbf{p_8}$,p_9,p_{10}), g_4 (p_{11}), g_5(p_{12}), g_6(p_{13}), g_7(p_{14}), g_8(0), g_9(p_{15}), g_{10}(p_{16}), for all sixteen parameters. The bolts are the lead parameters in groups with more than one population. In this case, all sixteen parameters could be represented by ten groups with parameters' correlations higher than 80% in each group. The weight factor of parameter p_1 is w_1=4/16, w_2=3/16 for p_5, w_8=0, and so on. However, it is possible to consider only the three first groups namely g_1($\mathbf{p_1}$,p_2,p_3,p_4), g_2($\mathbf{p_5}$,p_6,p_7) and g_3($\mathbf{p_8}$,p_9,p_{10}) covering only ten parameters out of sixteen, with confidence level of about 80% x 10/16 = 50%. Then the weight factors became w_1=4/10, w_2= w_3=3/10 for p_1, p_5, p_8, respectively. Each weighted lead parameter has a mean value of κ multiplied by its respective weight factor, and a unit standard deviation. This process does not alter the correlations among the parameters.
8. Composite matrix: A diagonal matrix of the normalized lead parameters as diagonal components was created. Other matrices, a matrix of correlation coefficients among the lead parameters and a diagonal matrix of the weight factors of the lead parameters were also constructed. The composite matrix is the product of these three matrices.
9. Composite-intensity index: The intensity of the earthquake event is measured by the strength of the composite matrix indicated by its norm. Any norm can be used and the simplest one, i.e., the Frobenius norm, was adopted in this study. This norm is referred to as the composite-intensity index in this study.
10. Damage state: As observed in Step 2, some seismic parameters are period-dependents. Hence the composite-intensity index in Step 9 is also period-dependent, and for an event there is a maximum composite-intensity index at a specific period as well as the associated MMI scale. The maximum composite-intensity indices for all events were then related to their respective MMI scales to produce

Table 1. The earthquake events, peak ground accelerations, peak ground velocities, and their origin.

No	Earthquake event	Station	PGA (g)			PGV (cm/s)			STATE
			1	2	UD	1	2	UD	
1	Tabas, 1978	Tabas	0.98	0.90	0.75	104	115	37	Iran
2	Erzinican, 1992	Erzinican	0.46	0.45	0.24	68	130	33	Turkey
3	Landers, 1992	Lucerene	0.80	0.71	0.86	35	94	47	USA
4	Northridge, 1994	Rinaldi	0.90	0.41	0.86	180	82	48	USA
5	Kobe, 1995	Takatori	0.80	0.43	0.16	189	75	22	Japan
6	Mexico, 2010	Michoacan	0.54	0.41	0.80	63	51	17	Mexico
7	Imperial Valley 7, 1979	El Centro 6	0.28	0.16	0.08	27	14	2	USA
8	Imperial Valley 6, 1979	Calexico	0.28	0.20	0.19	18	16	6	USA
9	Kobe, 1995	Amagasaki	0.33	0.29	0.34	49	39	28	Japan
10	Mammoth Lakes, 1980	Mammoth Lakes	0.44	0.39	0.26	26	26	10	USA
11	N Palm Spring, 1986	N Palm Springs 529	0.71	0.67	0.38	72	34	13	USA
12	Parkfield, 1966	Temblor	0.36	0.27	0.14	23	15	6	USA
13	Big Bear, 1992	Civic Center	0.55	0.48	0.20	37	29	13	USA
14	Hawai, 2006	Waimea	1.09	0.68	0.75	38	28	19	USA
15	L'Aquila, 2009	V. Aterno	0.68	0.57	0.51	41	43	15	Italy
16	New Zealand, 2010	Greendale	0.77	0.72	1.26	112	117	35	New Zealand
17	San Simeon, 2003	Templeton Hsptl	0.48	0.44	0.27	29	33	18	USA
18	Anchorage Alaska, 2018	St Fish & Game	0.48	0.19	0.17	36	19	9	USA
19	South Napa, 2014	Crockett #1	0.99	0.54	0.37	22	11	8	USA
20	Managua, 1972	Managua ESSO	0.37	0.33	0.31	33	33	19	Nicaragua
21	Chile, 2010	Angol	0.93	0.68	0.28	31	44	22	Chile
22	Cape Mendocino, 1992	Ferndale	0.38	0.27	0.07	97	47	7	USA
23	Loma Prieta, 1989	Capitola	0.51	0.44	0.56	42	28	17	USA
24	Calexico, 2010	Meloland Rd.	0.28	0.20	0.24	41	34	10	USA
25	Ferndale, 2010	Eureka & Dolbeer	0.33	0.23	0.08	32	17	5	USA
26	Imperial Valley, 1940*	El Centro Array 6	0.19	0.14	0.10	66	30	32	USA
27	Morgan Hill, 1984*	Gilroy	0.66	0.39	0.34	29	32	17	USA
28	N Palm Spring, 1986*	DHSP 517	0.59	0.57	0.28	40	63	25	USA
29	Chile Llolleo, 1985*	Llolleo	0.70	0.67	0.19	48	37	13	Chile
30	Chile Vina Del Mar, 1985*	Vina Del Mar	0.54	0.39	0.17	61	34	20	Chile
31	Mexico, 1995*	Mexico City	0.17	0.10	0.09	59	38	29	Mexico

* Two-horizontal component only. The vertical component was constructed as two thirds of the average of the horizontal components.

Diterima 8 Oktober 2021, Direvisi 31 Maret 2022, Diterima untuk dipublikasikan 25 April 2022

regression constants. The constants express the relation between the maximum composite-intensity index and the damaging power of the event. (Note: The MMI scales define its scales to the extent of damage of buildings subjected to an earthquake event.) Because the composite-intensity index is period-dependent then the damage state at any period can be accordingly computed; so is the MMI scales based on the regression constants.

These steps were elucidated in the following sections and started with the ground motions analyses considered in the study.

3. Ground Motion Records

For the investigation in this study, a total of thirty-one earthquake ground motions collected worldwide, mostly from the United States, were compiled. The number was immaterial, and the data set was by no means exhaustive, but the statistical significance was expected to be satisfied. They consisted of twenty-five three-component and six two-component strong earthquake records. For the latter, the vertical component was constructed as two-thirds of the average of the two horizontal components. They are all the strong earthquakes in character with the modified Mercalli intensity scales of VII-X and were listed in **Table 1**. To verify the statistical independence of the data, the cross-correlation coefficients were computed for all ninety-three components. The maximum correlation was 0.67 given by the Mexico 1995 earthquake between horizontal-1 and -2 components; all other values were less than this.

4. Earthquake Parameters And Their Correlation Coefficients

The dynamical equation of motion of a mass in three-orthogonal coordinate system is

$$\mathbf{M}\,\ddot{\mathbf{u}}(t)+\mathbf{C}\,\dot{\mathbf{u}}(t)+\mathbf{K}\,\mathbf{u}(t)=-\mathbf{M}\,\ddot{\mathbf{u}}_g(t) \tag{1}$$

where **M**, **C**, and **K** are 3 x 3 diagonal matrices of mass, damping, and stiffness, respectively; and $\ddot{\mathbf{u}}$, $\dot{\mathbf{u}}$, and **u** are the acceleration, velocity, and displacement vectors of the mass. For isotropic system, **Eq.** (**1**) reduces to,

$$\ddot{\mathbf{u}}(t)+2\zeta\omega_n\,\dot{\mathbf{u}}(t)+\omega_n^{\,2}\,\mathbf{u}(t)=-\ddot{\mathbf{u}}_g(t) \tag{2}$$

where $\ddot{\mathbf{u}}g$ =üg1, üg2, üg3 is the three-component translational ground acceleration vector, ζ is the damping, and ω_n is the system's natural frequency. The Duhamel integral solution of **Eq.** (**2**) for displacement vector is,

$$\mathbf{u}(t,\omega_n,\zeta)=-\frac{1}{\omega_D}\int_0^t \ddot{\mathbf{u}}_g(\tau)\,e^{-\zeta\omega_n(t-\tau)}\sin\omega_D(t-\tau)\,d\tau \tag{3}$$

Where

$$\omega_D=\omega_n\sqrt{1-\zeta^2}$$

The following earthquake parameters of a total of nineteen which were mostly developed based on **Eq.** (**3**) were investigated. The displacement spectrum is,

$$S_d(\omega_n,\zeta)=\max|\mathbf{u}(\omega_n,\zeta,t)| \tag{4}$$

Where $|\mathbf{u}|=\sqrt{\mathbf{u}\cdot\mathbf{u}}$. Similarly, velocity and acceleration spectra are defined as,

$$S_v(\omega_n,\zeta)=\max|\dot{\mathbf{u}}(\omega_n,\zeta,t)| \tag{5}$$

$$S_a(\omega_n,\zeta)=\max|\ddot{\mathbf{u}}(\omega_n,\zeta,t)+\ddot{\mathbf{u}}_g(t)| \tag{6}$$

Peak ground displacement, velocity, and acceleration are defined by,

$$\text{PGD}=\max|\mathbf{u}_g(t)|=\lim_{\omega_n\to 0}S_d(\omega_n,\zeta) \tag{7}$$

$$\text{PGV}=\max|\dot{\mathbf{u}}_g(t)|=\lim_{\omega_n\to 0}S_v(\omega_n,\zeta) \tag{8}$$

$$\text{PGA}=\max|\ddot{\mathbf{u}}_g(t)|=\lim_{\omega_n\to\infty}S_a(\omega_n,\zeta)=gA_0 \tag{9}$$

where g is the gravitational acceleration and A_0 is the peak ground acceleration coefficient.

The Housner spectrum intensity, $SI(\zeta)$ (Housner, 1952), and seismic energy density, $SED(\zeta)$, which is the average of the absorbed energy per unit mass, are defined as,

$$SI(\zeta)=\int_{0.1}^{2.5}S_{pv}(T,\zeta)\,dT \tag{10}$$

$$SED(\zeta)=\int_{T_1}^{T_2}\frac{S_{pv}^2(T,\zeta)}{|T_2-T_1|}\,dT \tag{11}$$

where $S_{pv}(\omega_n,\zeta)=\omega_n S_d(\omega_n,\zeta)$ is the pseudo-velocity spectrum; and the damping is taken to be ζ=5%, T_1=0.1, T_2=2.5 seconds.

The Arias intensity (Arias, 1970) is defined as,

$$I_A=\frac{\pi}{2g}\int_0^{t_d}|\ddot{\mathbf{u}}_g(t)|^2\,dt \tag{12}$$

where t_d is the end-time of the record.
Campbell and Bozorgnia (2012) investigated the cumulative absolute velocity (*CAV*) extensively. They related *CAV* to the macroseismic intensities I_{MM} (US), I_{JMA} (Japan), and I_{EMS} (Europe). They suggested that *CAV* was the most stable IM to correlate with damage potentials. There were some others who also studied this *CAV* or its variants (e.g., Kramer and Mitchell, 2006). A slightly different version, denoted herein as CAV_{MM}, is investigated, and defined as,

$$CAV_{MM}=g\int_0^{t_d}H\left(\frac{|\ddot{\mathbf{u}}_g(t)|}{g}-0.025\right)\frac{|\ddot{\mathbf{u}}_g(t)|}{g}\,dt \tag{13}$$

where H is the Heaviside step function,

$$H\left(\frac{|\ddot{\mathbf{u}}_g(t)|}{g}-0.025\right)=\begin{cases}1 & \text{when } \dfrac{|\ddot{\mathbf{u}}_g(t)|}{g}\geq 0.025\\ 0 & \text{when } \dfrac{|\ddot{\mathbf{u}}_g(t)|}{g}<0.025\end{cases} \tag{14}$$

The corner period, T_c, is the one at which the constant acceleration intersects the constant velocity pseudo-spectra, and defined by,

Diterima 8 Oktober 2021, Direvisi 31 Maret 2022, Diterima untuk dipublikasikan 25 April 2022

$$T_c = 2\pi \frac{S_{pv\max}}{S_{pa\max}} \quad (15)$$

where $S_{pa}(\omega_n,\zeta) = \omega_n S_{pv}(\omega_n,\zeta)$ is the pseudo-acceleration spectrum.

The power per unit mass absorbed by the damping and the spring, $P_a(T,\zeta)/m$, and the power excited by the ground motion to the system, $P_{in}(T,\zeta)/m$, are expressed as,

$$P_a(T,\zeta)/m = \max\left|\ddot{\mathbf{u}}_t(T,\zeta,t)\cdot\dot{\mathbf{u}}(T,\zeta,t)\right| \quad (16)$$

$$P_{in}(T,\zeta)/m = \max\left|\ddot{\mathbf{u}}_t(T,\zeta,t)\cdot\dot{\mathbf{u}}_g(t)\right| \quad (17)$$

where m is the mass of the oscillator; and, thereby the input energy density, $E_{in}(T,\zeta)/m$, becomes,

$$E_{in}(T,\zeta)/m = \Delta t\sum_{t=0}^{t_d}\ddot{\mathbf{u}}_t(T,\zeta,t)\cdot\dot{\mathbf{u}}_g(t) \quad (18)$$

where the total ground acceleration is $\ddot{\mathbf{u}}_t(t) = \ddot{\mathbf{u}}(t) + \ddot{\mathbf{u}}_g(t)$, Δt is the time interval, and t_d is the end-time of the record.

The time parameters consist of the significant duration $D_{05\text{-}95}$ (Trifunac and Brady, 1975), bracketed duration, and elapse are defined as follows (see **Figure 1** for elaboration).

$$D_{05-95} = t(I_{NA}=0.95) - t(I_{NA}=0.05) \quad (19)$$

$$Duration = t(R_g=\sigma\,|\,out) - t(R_g=\sigma\,|\,in) \quad (20)$$

Elapse = total vibration of the record (21)

where

$$R_g = \left|\ddot{\mathbf{u}}_g\right| = \sqrt{\ddot{u}_{g1}{}^2 + \ddot{u}_{g2}{}^2 + \ddot{u}_{g3}{}^2}$$

$$\sigma = \sqrt{\frac{1}{n}\sum_{i=1}^{n} R_{gi}{}^2}$$

and I_{NA} is the normalized Arias intensity. **Eq. (19)** simply states that $D_{05\text{-}95}$ is equal to the time range between the attainment of 5% of the Arias intensity and that of 95%. And **Eq. (20)** specifies duration as the time range between the acceleration hit the standard deviation at the incoming and at the outgoing points. **Figure 1** graphically elaborates **Eqs. (19)-(21)**.

Besides those referred to in Eqs. (4)-(21), two more parameters A_0T_c, which is a measure of a characteristic velocity, and MMI (the modified Mercalli intensity, Wood and Neumann, 1931) were considered, completing nineteen. The MMI was determined in accordance with Wald *et. al.* (1999). Notice that some of the parameters investigated in this study were period -dependents while the others were not. For those that were period-dependents, their values were evaluated at T=0.1-1.0 seconds with increment of 0.1 seconds; T =1.0-3.0 seconds with increment of 0.2 seconds; and T =3.0-5.0 seconds with increment of 0.5 seconds, totalling twenty-four periods. However, due to space limitation only computations for T =1.0 second were presented in the paper. The results of the nineteen parameters computations for thirty-one earthquakes at T =1.0 second were presented in **Table 2**. Next, the correlation coefficients of all earthquake parameters listed in **Table 2** were determined.

The expression for the Pearson correlation coefficient between any two normal random variables is expressible as (e.g., Ang and Tang, 2007),

$$\rho_{XY} = \frac{E[(x-\mu_X)(y-\mu_Y)]}{\sigma_X\,\sigma_Y} \quad (22)$$

where ρ_{XY} is the correlation coefficient of parameters X,Y; E is the ensemble average, and σ, μ are the standard deviation and the mean value, respectively. Employing **Eq. (22)** to all nineteen earthquake parameters, the resulting values were presented in **Table 3**. The table presented the correlation coefficients of the common logarithm of the earthquake parameters which were assumed lognormally distributed.

In **Table 3** there are three-pair parameters that are fully correlated with the others (in grey), i.e., SI and SED, P_a/m and S_v, as well as S_d and S_a; and this is true for all periods investigated in the study. Therefore SED, P_a/m, and S_d were dropped from further analyses to avoid double counting; thus, the remaining parameters become sixteen. From the table, the parameters with correlation coefficients of 0.8 or higher were collected and listed in **Table 4**. For illustration, in the first row, $S_a(T=1)$ was correlated with $S_v(T=1)$, $P_{in}(T=1)/m$, $E_{in}(T=1)/m$ as high as 0.96, 0.96, 0.94, respectively (see

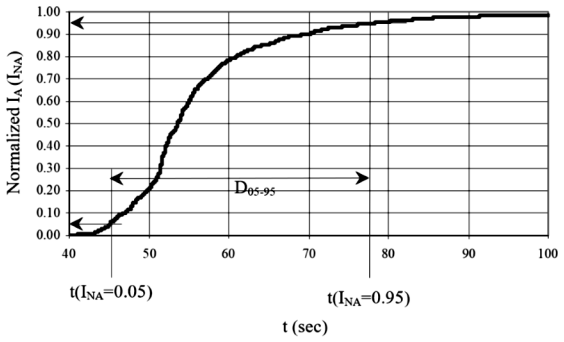

(a) The normalized arias intensity vs time to define $D_{05\text{-}95}$

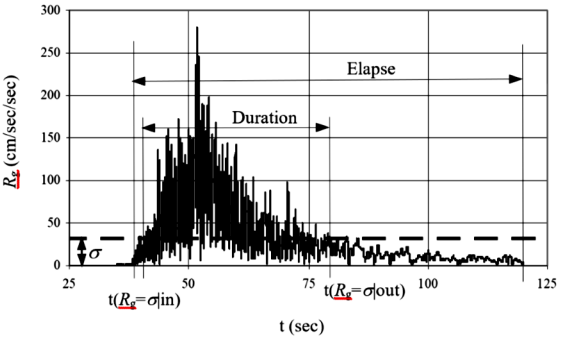

(b) The amplitude of the ground motion vs time to define duration and elapse

$$R_g = \left|\ddot{\mathbf{u}}_g\right| = \sqrt{\ddot{u}_{g1}{}^2 + \ddot{u}_{g2}{}^2 + \ddot{u}_{g3}{}^2} \qquad \sigma = \sqrt{\frac{1}{n}\sum_{i=1}^{n} R_{gi}{}^2}$$

Figure 1. Definition of duration used in the study

Diterima 8 Oktober 2021, Direvisi 31 Maret 2022, Diterima untuk dipublikasikan 25 April 2022

Table 2. Values of the earthquake parameters at period *T*=1.0 second.

No	Earthquake event	CAV_{MM}	PGA	PGV	PGD	I_{MM}	I_A	T_c	A_0T_c	Elapse	Duration	D_{05-95}	SI	SED	$S_a(1)$	$S_v(1)$	$S_d(1)$	$P_a/m(1)$	$P_{in}/m(1)$	$E_{in}/m(1)$
		g-s	cm/s^2	cm/s	cm		m/s	s	s	s	s	s	m	m^2/s^2	cm/s^2	cm/s	cm	hp/ton	hp/ton	m^2/s^2
		1	2	3	4	5	6	7	8	9	10	11	12	13	14	15	16	17	18	19
1	Tabas, 1978	6.40	1,207	133	93	IX	32.3	0.66	0.82	90	21	16	3.68	2.70	761	137	19.1	7.2	8.9	6.27
2	Erzinican, 1992	1.70	494	133	47	VIII	4.5	1.19	0.60	33	9	10	3.27	2.27	985	146	24.9	8.2	6.8	1.73
3	Landers, 1992	4.42	877	107	39	IX	21.5	0.37	0.33	25	16	12	2.30	1.11	568	78	14.4	2.4	2.3	0.88
4	Northridge, 1994	3.11	960	183	36	IX	16.7	0.68	0.66	25	10	8	5.29	5.88	1,966	316	49.6	40.6	21.7	8.68
5	Kobe, 1995	3.46	794	190	55	X	15.4	1.21	0.98	35	12	11	6.97	11.47	1,637	232	41.3	26.1	12.6	11.58
6	Mexico, 2010	3.31	813	81	39	IX	18.2	0.34	0.28	60	37	32	2.22	1.01	712	115	17.9	5.1	2.7	3.39
7	Imperial Valley 7, 1979	0.23	282	27	3	VII	0.4	0.38	0.11	20	5	3	0.59	0.08	213	40	5.3	0.8	0.6	0.10
8	Imperial Valley 6, 1979	1.25	283	19	8	VII	2.1	0.53	0.15	30	15	11	0.86	0.15	218	36	5.5	0.5	0.5	0.26
9	Kobe, 1995	2.08	367	58	30	VIII	4.7	1.02	0.38	45	17	13	2.64	1.56	952	150	24.0	10.1	4.0	4.43
10	Mammoth Lakes, 1980	0.76	504	33	4	VII	2.3	0.22	0.11	20	4	3	0.77	0.12	171	37	4.3	0.5	0.5	0.08
11	N Palm Spring, 1986	1.28	722	79	18	IX	4.5	0.44	0.33	15	7	6	2.65	1.46	815	124	20.5	8.3	4.7	1.88
12	Parkfield, 1966	0.41	371	24	5	VII	0.8	0.38	0.14	34	6	5	0.60	0.08	203	35	5.1	0.5	0.6	0.14
13	Big Bear, 1992	2.14	628	37	7	VIII	6.6	0.32	0.20	25	13	10	0.94	0.21	216	40	5.4	0.6	0.5	0.19
14	Hawai, 2006	4.94	1,111	43	4	VIII	26.7	0.21	0.01	37	13	10	0.99	0.27	243	50	6.1	1.1	0.9	0.24
15	L'Aquila, 2009	1.74	759	47	7	VIII	5.7	0.29	0.22	21	9	8	1.51	0.46	453	86	11.4	2.6	1.6	0.61
16	New Zealand, 2010	4.09	1,357	156	82	X	20.5	0.69	0.95	45	24	11	4.94	5.23	1,116	193	28.2	13.5	16.0	4.49
17	San Simeon, 2003	1.56	532	37	11	VIII	4.2	0.33	0.18	19	10	12	1.43	0.40	453	69	11.4	1.8	2.1	0.90
18	Anchorage Alaska, 2018	1.64	468	38	12	VIII	3.2	0.57	0.27	30	13	13	1.18	0.31	473	79	11.9	2.7	1.7	0.83
19	South Napa, 2014	0.66	981	24	2	VIII	2.6	0.14	0.14	26	3	3	0.46	0.07	108	37	2.7	0.3	0.3	0.06
20	Managua, 1972	1.68	423	34	10	VIII	4.8	0.34	0.15	23	9	8	1.34	0.36	409	76	10.3	2.7	1.4	0.80
21	Chile, 2010	9.82	1,093	44	38	VIII	40.8	0.18	0.20	85	59	47	1.56	0.48	486	84	12.2	2.5	2.0	2.28
22	Cape Mendocino, 1992	1.49	393	97	28	VIII	3.1	1.31	0.53	30	13	12	2.77	1.65	766	120	19.3	6.7	3.8	1.74
23	Loma Prieta, 1989	2.95	655	46	8	VIII	11.2	0.45	0.30	31	12	11	2.07	0.94	559	83	14.1	2.8	1.5	1.17
24	Calexico, 2010	2.99	281	44	44	VIII	4.4	0.79	0.23	100	49	37	1.23	0.30	369	60	9.3	1.7	1.3	0.95
25	Ferndale, 2010	0.75	325	33	10	VII	1.2	0.44	0.15	40	16	10	1.08	0.24	379	64	9.6	1.7	1.2	0.70
26	Imperial Valley, 1940	0.80	221	76	33	IX	1.3	2.85	0.64	25	9	7	1.72	0.80	291	41	7.4	0.8	2.0	0.18
27	Morgan Hill, 1984	2.36	808	41	9	VIII	6.0	0.30	0.25	65	17	16	1.84	0.66	562	107	14.2	3.5	2.2	2.83
28	North Palm Spring, 1986	1.96	682	68	16	VIII	7.1	0.28	0.20	40	10	7	2.21	0.94	680	92	17.1	4.7	2.9	1.34
29	Chile Llolleo, 1985	8.90	781	51	11	VIII	33.9	0.36	0.28	100	39	35	2.40	1.16	745	143	18.8	5.5	3.1	4.73
30	Chile Vina Del Mar, 1985	7.86	595	64	9	VIII	24.5	0.72	0.44	100	51	43	2.66	1.70	1,093	189	27.5	13.9	6.3	13.58
31	Mexico, 1995	2.99	209	71	27	VIII	4.3	2.03	0.43	90	43	34	3.28	3.94	281	32	7.1	0.6	1.4	0.38

Table 3). Therefore, they constituted the first group of four elements (see the first row of **Table 4**). The next group in second row, D_{05-95} was correlated with duration and elapse as high as 0.96 and 0.82; and therefore, they formed the second group. This went on to the next row or group (each row constituted a group) in **Table 4**. In the table each column can only be occupied by one parameter; when there was more than one then the lower in the hierarchy was ignored. The columns in grey denoted the dropped parameters due to their full correlation with the others. For this period some lead parameters were determined. For instance, S_a was the lead parameter for the other three parameters in checkmarks (see the table's first row) with a correlation coefficient of 0.8 or higher. Therefore, S_a became the first lead parameter for *T*=1.0 second. The second lead parameter was D_{05-95} which represented two other parameters. The third lead parameter was the PGV which represented two other parameters. The fourth, fifth, sixth, and seventh were I_A, I_{MM}, T_c, and A_0T_c, which was the lead parameter to itself; similarly for ninth and tenth. The total parameters represented by these ten lead parameters were sixteen, all with a correlation coefficient of 0.8 or higher. This step was repeated for other periods totalling twenty-four.

The next step is to perform the counting of each parameter for all twenty-four periods. For illustration, S_a counts twenty-four times as the first lead parameter over all twenty-four periods, and in total it represented 106 parameters including itself (detail calculation not shown); D_{05-95} counts twenty-four times as the second lead parameter and represented 72 parameters; and so on. The record was documented in **Table 5**. This is carried out for all ten parameters. The numbers of the represented parameters were indicated at the rightmost column. The total counts must be 16 (parameters) x 24 (periods) = 384 (right bottom). **Table 5** showed that to characterize all thirty-one earthquakes completely it takes ten parameters with correlation coefficients of 0.8 or higher. Now, it is the interest to take the fewest parameters to characterize the earthquakes even with lower representation.

The indexing of each parameter was carried out, for instance for S_a, based on **Table 5**. As the first lead parameter, S_a was given an index of its respective counts (24) divided by the total (24) and multiplied by the number this first lead parameter represented (106) (see **Table 5**) or 24/24 x 106 = 106 and was documented in **Table 6**. And as the second lead

Diterima 8 Oktober 2021, Direvisi 31 Maret 2022, Diterima untuk dipublikasikan 25 April 2022

Table 3. Correlation coefficients among common logarithm of earthquake parameters at period *T*=1.0 second. Fully correlated parameters are in grey.

Log		CAV_{MM}	PGA	PGV	PGD	I_{MM}	I_A	T_c	A_0T_c	Elapse	Duration	D_{05-95}	SI	SED	$S_a(1)$	$S_v(1)$	$S_d(1)$	$P_a/m(1)$	$P_{in}/m(1)$	$E_{in}/m(1)$
Log		**1**	**2**	**3**	**4**	**5**	**6**	**7**	**8**	**9**	**10**	**11**	**12**	**13**	**14**	**15**	**16**	**17**	**18**	**19**
CAV_{MM}	1	1.00	0.44	0.55	0.53	0.47	0.79	0.13	0.25	0.62	0.65	0.63	0.61	0.61	0.51	0.51	0.51	0.50	0.51	0.62
PGA	2	0.44	1.00	0.37	0.16	0.52	0.76	-0.51	0.03	0.09	0.07	0.08	0.31	0.29	0.37	0.52	0.37	0.44	0.39	0.42
PGV	3	0.55	0.37	1.00	0.82	0.82	0.54	0.53	0.69	0.15	0.25	0.24	0.92	0.92	0.81	0.75	0.81	0.78	0.89	0.70
PGD	4	0.53	0.16	0.82	1.00	0.71	0.47	0.59	0.71	0.38	0.53	0.51	0.81	0.80	0.71	0.60	0.71	0.64	0.78	0.68
I_{MM}	5	0.47	0.52	0.82	0.71	1.00	0.60	0.33	0.59	0.09	0.23	0.24	0.76	0.77	0.64	0.63	0.64	0.63	0.73	0.59
I_A	6	0.79	0.76	0.54	0.47	0.60	1.00	-0.13	0.19	0.49	0.60	0.62	0.59	0.58	0.57	0.61	0.57	0.57	0.55	0.68
T_c	7	0.13	-0.51	0.53	0.59	0.33	-0.13	1.00	0.65	0.16	0.23	0.23	0.56	0.59	0.38	0.23	0.39	0.30	0.47	0.29
$A_0 T_c$	8	0.25	0.03	0.69	0.71	0.59	0.19	0.65	1.00	0.18	0.24	0.25	0.74	0.73	0.65	0.58	0.65	0.58	0.69	0.60
Elapse	9	0.62	0.09	0.15	0.38	0.09	0.49	0.16	0.18	1.00	0.85	0.82	0.29	0.30	0.23	0.22	0.23	0.21	0.24	0.47
Duration	10	0.65	0.07	0.25	0.53	0.23	0.60	0.23	0.24	0.85	1.00	0.96	0.42	0.42	0.38	0.31	0.38	0.31	0.34	0.58
D_{05-95}	11	0.63	0.08	0.24	0.51	0.24	0.62	0.23	0.25	0.82	0.96	1.00	0.43	0.43	0.39	0.33	0.39	0.32	0.34	0.59
SI	12	0.61	0.31	0.92	0.81	0.76	0.59	0.56	0.74	0.29	0.42	0.43	1.00	1.00	0.90	0.82	0.90	0.85	0.93	0.85
SED	13	0.61	0.29	0.92	0.80	0.77	0.58	0.59	0.73	0.30	0.42	0.43	1.00	1.00	0.87	0.78	0.87	0.82	0.91	0.81
$S_a(1)$	14	0.51	0.37	0.81	0.71	0.64	0.57	0.38	0.65	0.23	0.38	0.39	0.90	0.87	1.00	0.96	1.00	0.98	0.96	0.94
$S_v(1)$	15	0.51	0.52	0.75	0.60	0.63	0.61	0.23	0.58	0.22	0.31	0.33	0.82	0.78	0.96	1.00	0.96	1.00	0.92	0.93
$S_d(1)$	16	0.51	0.37	0.81	0.71	0.64	0.57	0.39	0.65	0.23	0.38	0.39	0.90	0.87	1.00	0.96	1.00	0.98	0.96	0.94
$P_a/m(1)$	17	0.50	0.44	0.78	0.64	0.63	0.57	0.30	0.58	0.21	0.31	0.32	0.85	0.82	0.98	1.00	0.98	1.00	0.94	0.93
$P_{in}/m(1)$	18	0.51	0.39	0.89	0.78	0.73	0.55	0.47	0.69	0.24	0.34	0.34	0.93	0.91	0.96	0.92	0.96	0.94	1.00	0.89
$E_{in}/m(1)$	19	0.62	0.42	0.70	0.68	0.59	0.68	0.29	0.60	0.47	0.58	0.59	0.85	0.81	0.94	0.93	0.94	0.93	0.89	1.00

Table 4. For each row, the representativelead parameter (in black squared) and the represented parameters (checked marks) with correlation coefficients of 0.8 or higher at period T=1.0 second. SED, S_d, and P_a/m have been dropped to avoid double counting (in grey).

T	CAV_{MM}	PGA	PGV	PGD	I_{MM}	I_A	T_c	A_0T_c	Elapse	Duration	D_{05-95}	SI	SED	S_a	S_v	S_d	P_a/m	P_{in}/m	E_{in}/m	Sum	Total
s	**1**	**2**	**3**	**4**	**5**	**6**	**7**	**8**	**9**	**10**	**11**	**12**	**13**	**14**	**15**	**16**	**17**	**18**	**19**		
1	0	0	0	0	0	0	0	0	0	0	0	0	0	**1**	√	0	0	√	√	4	16
	0	0	0	0	0	0	0	0	√	√	**2**	0	0	0	0	0	0	0	0	3	
	0	0	**3**	√	0	0	0	0	0	0	0	√	0	0	0	0	0	0	0	3	
	0	0	0	0	0	**4**	0	0	0	0	0	0	0	0	0	0	0	0	0	1	
	0	0	0	0	**5**	0	0	0	0	0	0	0	0	0	0	0	0	0	0	1	
	0	0	0	0	0	0	**6**	0	0	0	0	0	0	0	0	0	0	0	0	1	
	0	0	0	0	0	0	0	**7**	0	0	0	0	0	0	0	0	0	0	0	1	
	0	0	0	0	0	0	0	0	0	0	0	0	0	0	0	0	0	0	0	0	
	0	**9**	0	0	0	0	0	0	0	0	0	0	0	0	0	0	0	0	0	1	
	10	0	0	0	0	0	0	0	0	0	0	0	0	0	0	0	0	0	0	1	

Table 5. The non-zero counting of lead parameters for all twenty-four periods and their represented parameters including itself.

The lead parameter	PGA	PGV	I_{MM}	I_A	T_c	D_{05-95}	S_a	P_{in}/m	A_0T_c	CAV_{MM}	Total	The number of the represented Parameters including itself
1	0	0	0	0	0	0	24	0	0	0	24	106
2	0	0	0	0	0	24	0	0	0	0	24	72
3	0	24	0	0	0	0	0	0	0	0	24	61
4	0	0	0	24	0	0	0	0	0	0	24	24
5	0	0	24	0	0	0	0	0	0	0	24	24
6	0	0	0	0	24	0	0	0	0	0	24	24
7	0	0	0	0	0	0	0	0	24	0	24	24
8	0	0	0	0	0	0	0	4	0	0	4	4
9	21	0	0	0	0	0	0	0	0	0	21	21
10	0	0	0	0	0	0	0	0	0	24	24	24
Total	21	24	24	24	24	24	24	4	24	24	217	384

parameter D_{05-95} was indexed as 24/24 x 72 = 72. Continued, this was performed for all ten parameters. The index sum for S_a was therefore 106 or merely 27.60% of 384 populations (see bottom row of **Table 6** under S_a). All other lead parameters were indexed similarly. The bottom row indicated that there was no

Diterima 8 Oktober 2021, Direvisi 31 Maret 2022, Diterima untuk dipublikasikan 25 April 2022

Table 6. The index of the represented parameter including itself.

The most representative parameter	PGA	PGV	I_{MM}	I_A	T_c	D_{05-95}	S_a	P_{in}/m	A_0T_c	CAV_{MM}	Total
1	0	0	0	0	0	0	106	0	0	0	106
2	0	0	0	0	0	72	0	0	0	0	72
3	0	61	0	0	0	0	0	0	0	0	61
4	0	0	0	24	0	0	0	0	0	0	24
5	0	0	24	0	0	0	0	0	0	0	24
6	0	0	0	0	24	0	0	0	0	0	24
7	0	0	0	0	0	0	0	0	24	0	24
8	0	0	0	0	0	0	0	4	0	0	4
9	21	0	0	0	0	0	0	0	0	0	21
10	0	0	0	0	0	0	0	0	0	24	24
Total	21	61	24	24	24	72	106	4	24	24	384
Percentage	5.47%	**15.89%**	6.25%	6.25%	6.25%	**18.75%**	**27.60%**	1.04%	6.25%	6.25%	100%

Table 7. S_a, D_{05-95}, PGV (in black cells) and their represented parameters (checked cells) with correlation coefficients 0.8 or higher for *T*=1.0 second. The grey cells indicate non-represented parameters in the scenario.

T	CAV_{MM}	PGA	PGV	PGD	I_{MM}	I_A	T_c	A_0T_c	Elapse	Duration	D_{05-95}	SI	S_a	S_v	P_{in}/m	E_{in}/m	Out of 16	Percent	
s	1	2	3	4	5	6	7	8	9	10	11	12	13	14	15	16			
	0	0	0	0	0	0	0	0	0	0	0	0	**1**	√	√	√	4	25%	
1.0	0	0	0	0	0	0	0	0	√	√	**2**	0	0	0	0	0	3	19%	63%
	0	0	**3**	√	0	0	0	0	0	0	0	√	0	0	0	0	3	19%	

Table 8. The statistical values employed in the normalization process for thirty-one earthquake records

T (s)	S Log $S_a(T)$	S $[\text{Log } S_a(T)]^2$	T (s)	Σ Log $S_a(T)$	Σ $[\text{Log } S_a(T)]^2$
0.1	94	288	1.6	76	192
0.2	96	299	1.8	75	184
0.3	96	296	2.0	73	178
0.4	93	282	2.2	72	171
0.5	91	271	2.4	71	167
0.6	90	260	2.6	69	160
0.7	88	250	2.8	68	154
0.8	86	243	3.0	66	147
0.9	85	235	3.5	63	135
1.0	83	227	4.0	60	122
1.2	81	215	4.5	55	106
1.4	78	202	5.0	52	94

Σ Log D_{05-95}	=	33
Σ $[\text{Log } D_{05-95}]^2$	=	38
Σ Log PGV	=	54
Σ $[\text{Log PGV}]^2$	=	97
Scale factor	=	2.3741

single lead parameter sufficient to characterize all thirty-one earthquakes; S_a represented merely 27.60%, next was D_{05-95} with 18.75%, and PGV of 15.89%, totalling 62.24%. Hence, it was clear from the table that characterizing earthquake ground motions with less than those three parameters (namely the spectral acceleration, duration, and peak ground velocity) would not be sufficient. This agreed with the cases reported by other investigators (Bijukchhen *et. al.*, 2017, Goto and Morikawa, 2012, Wu *et. al.*, 2012). Moreover, **Table 6** also showed that PGA was a poor indicator of damage as agreed with other views (Wu *et. al.*, 2003, Sandeep and Prasad, 2012). It was hoped sufficient to characterize the earthquakes based on these three lead parameters with the coefficients of correlation 0.8 or higher. In what follows the details of S_a, D_{05-95}, PGV parameters were investigated.

Table 7 for S_a, D_{05-95} and PGV were processed in a similar manner with **Table 4**. For instance, at period *T*=1.0 second, S_a represented four parameters including itself, three parameters for D_{05-95} and another three parameters for PGV, totaling ten, or 63% of sixteen parameters. The remaining 37% non-represented were CAV_{MM}, PGA, I_{MM}, I_A, T_c, and A_0T_c in grey. Overall, the minimum percentage of the represented parameters was 56%, and the maximum 63%. Because the correlation among the parameters was 0.8 or higher, then the confidence level became 45-50%, or about the median level. In total, five parameters CAV_{MM}, I_{MM}, I_A, T_c, and A_0T_c were never represented in this scenario.

5. Composite-Intensity Index Spectrum

Because most variables have different units then a change of variable was introduced to convert the problem into dimensionless values. In the conversion, to minimize the biases, their mean values were set to a specific value, κ. The value of κ was determined so that after the conversion, the normalized values were

Diterima 8 Oktober 2021, Direvisi 31 Maret 2022, Diterima untuk dipublikasikan 25 April 2022

Table 9. The period-dependent correlation coefficients and weight factors of Log S_a′, Log PGV′, and Log $D_{05\text{-}95}$′ for twenty-four periods.

	Log/Log	S_a	$D_{05\text{-}95}$	PGV		Log/Log	S_a	$D_{05\text{-}95}$	PGV		Log/Log	S_a	$D_{05\text{-}95}$	PGV
T=0.1 sec	S_a	1.00	-0.05	0.24	T=0.2 sec	S_a	1.00	0.06	0.19	T=0.3 sec	S_a	1.00	-0.15	0.19
	$D_{05\text{-}95}$	-0.05	1.00	0.24		$D_{05\text{-}95}$	0.06	1.00	0.24		$D_{05\text{-}95}$	-0.15	1.00	0.24
	PGV	0.24	0.24	1.00		PGV	0.19	0.24	1.00		PGV	0.19	0.24	1.00
	Weight	0.40	0.30	0.30		Weight	0.40	0.30	0.30		Weight	0.40	0.30	0.30
T=0.4 sec	S_a	1.00	-0.03	0.20	T=0.5 sec	S_a	1.00	0.30	0.48	T=0.6 sec	S_a	1.00	0.37	0.58
	$D_{05\text{-}95}$	-0.03	1.00	0.24		$D_{05\text{-}95}$	0.30	1.00	0.24		$D_{05\text{-}95}$	0.37	1.00	0.24
	PGV	0.20	0.24	1.00		PGV	0.48	0.24	1.00		PGV	0.58	0.24	1.00
	Weight	0.40	0.30	0.30		Weight	0.40	0.30	0.30		Weight	0.40	0.30	0.30
T=0.7 sec	S_a	1.00	0.41	0.74	T=0.8 sec	S_a	1.00	0.39	0.78	T=0.9 sec	S_a	1.00	0.40	0.79
	$D_{05\text{-}95}$	0.41	1.00	0.24		$D_{05\text{-}95}$	0.39	1.00	0.24		$D_{05\text{-}95}$	0.40	1.00	0.24
	PGV	0.74	0.24	1.00		PGV	0.78	0.24	1.00		PGV	0.79	0.24	1.00
	Weight	0.40	0.30	0.30		Weight	0.40	0.30	0.30		Weight	0.40	0.30	0.30
T=1.0 sec	S_a	1.00	0.39	0.81	T=1.2 sec	S_a	1.00	0.40	0.85	T=1.4 sec	S_a	1.00	0.44	0.87
	$D_{05\text{-}95}$	0.39	1.00	0.24		$D_{05\text{-}95}$	0.40	1.00	0.24		$D_{05\text{-}95}$	0.44	1.00	0.24
	PGV	0.81	0.24	1.00		PGV	0.85	0.24	1.00		PGV	0.87	0.24	1.00
	Weight	0.40	0.30	0.30		Weight	0.40	0.30	0.30		Weight	0.40	0.30	0.30
T=1.6 sec	S_a	1.00	0.40	0.87	T=1.8 sec	S_a	1.00	0.41	0.88	T=2.0 sec	S_a	1.00	0.40	0.86
	$D_{05\text{-}95}$	0.40	1.00	0.24		$D_{05\text{-}95}$	0.41	1.00	0.24		$D_{05\text{-}95}$	0.40	1.00	0.24
	PGV	0.87	0.24	1.00		PGV	0.88	0.24	1.00		PGV	0.86	0.24	1.00
	Weight	0.50	0.30	0.20		Weight	0.50	0.30	0.20		Weight	0.50	0.30	0.20
T=2.2 sec	S_a	1.00	0.39	0.87	T=2.4 sec	S_a	1.00	0.41	0.86	T=2.6 sec	S_a	1.00	0.39	0.84
	$D_{05\text{-}95}$	0.39	1.00	0.24		$D_{05\text{-}95}$	0.41	1.00	0.24		$D_{05\text{-}95}$	0.39	1.00	0.24
	PGV	0.87	0.24	1.00		PGV	0.86	0.24	1.00		PGV	0.84	0.24	1.00
	Weight	0.50	0.30	0.20		Weight	0.50	0.30	0.20		Weight	0.50	0.30	0.20
T=2.8 sec	S_a	1.00	0.38	0.81	T=3.0 sec	S_a	1.00	0.34	0.80	T=3.5 sec	S_a	1.00	0.39	0.80
	$D_{05\text{-}95}$	0.38	1.00	0.24		$D_{05\text{-}95}$	0.34	1.00	0.24		$D_{05\text{-}95}$	0.39	1.00	0.24
	PGV	0.81	0.24	1.00		PGV	0.80	0.24	1.00		PGV	0.80	0.24	1.00
	Weight	0.50	0.30	0.20		Weight	0.50	0.30	0.20		Weight	0.50	0.30	0.20
T=4.0 sec	S_a	1.00	0.44	0.79	T=4.5 sec	S_a	1.00	0.43	0.79	T=5.0 sec	S_a	1.00	0.44	0.77
	$D_{05\text{-}95}$	0.44	1.00	0.24		$D_{05\text{-}95}$	0.43	1.00	0.24		$D_{05\text{-}95}$	0.44	1.00	0.24
	PGV	0.79	0.24	1.00		PGV	0.79	0.24	1.00		PGV	0.77	0.24	1.00
	Weight	0.50	0.30	0.20		Weight	0.50	0.30	0.20		Weight	0.50	0.30	0.20

positives. The following expression was used to normalize the normal random variable,

$$x' = \frac{x - \mu_X + \kappa \sigma_X}{\sigma_X} \geq 0 \quad (23)$$

where x' is the normalized random variable of x, and κ is a constant to be later. **Eq. (23)** yields mean values and standard deviations $\mu_{X'} = \kappa$ and $\sigma_{X'} = 1$. The values of the Σ Log $S_a(T)$, Σ Log $D_{05\text{-}95}$, Σ Log PGV, Σ [Log $S_a(T)$]^2, Σ [Log $D_{05\text{-}95}$]^2, Σ [Log PGV]^2 as shown in **Table 8** were employed in the normalization process of Log $S_a(T)$, Log $D_{05\text{-}95}$, and Log PGV by **Eq. (23)**, resulting in Log $S_a(T)$′, Log $D_{05\text{-}95}$′ and Log PGV′. Next, these three parameters were weighted by using the percentage of the right column of **Table 7**. For example, for T=1.0 second, the weight factors were w_a=25%/63%=0.40, w_d=19%/63%=0.30, w_v=19%/63%=0.30 for Log $S_a(T)$′, Log $D_{05\text{-}95}$′, and Log PGV′, respectively. (Their complete values covering all twenty-four periods were listed in **Table 9**.) Following this weighted averaging, the sum of all parameter-means and standard deviations became $\Sigma\mu_{X'} = \Sigma_i(w_i \kappa) = \kappa$ and $\Sigma\sigma_{X'} = \Sigma_i w_i = 1$, respectively. This operation and that of **Eq. (23)** did not alter the correlation coefficients computed by **Eq. (22)**.

A period dependent three-component diagonal matrix $\mathbf{C_D}(T)$=Diag[$C_{D1}(T)$,C_{D2},C_{D3}] with the weighted Log S_a (T)′, Log $D_{05\text{-}95}$ ′, and Log PGV′ as its diagonal components were created, i.e. $C_{D1}(T)$=$w_a(T)$ Log S_a (T)′, C_{D2}=w_d Log $D_{05\text{-}95}$′, C_{D3}=w_v Log PGV′. In fact, $\mathbf{C_D}(T)$ could be decomposed into $\mathbf{C_D}(T)$=$\mathbf{W_D}(T)\mathbf{C_D}(T)$′, where $\mathbf{W_D}(T)$=Diag[$w_a(T)$,w_d,w_v], is a weight factor diagonal matrix, and, similarly, $\mathbf{C_D}(T)$′=Diag[Log S_a (T)′, Log $D_{05\text{-}95}$′, Log PGV′]. The correlation coefficients were accounted for through matrix multiplication with $\mathbf{C_D}(T)$ to obtain $\mathbf{C}(T)$=$\mathbf{C_D}(T)\mathbf{r}(T)$= $\mathbf{W_D}(T)\mathbf{C_D}(T)'\mathbf{r}(T)$. The composite-index spectrum is defined as the strength of $\mathbf{C}(T)$ and was measured by its Frobenius norm, which can be expressed as (e.g., Ford, 2015),

$$I_{CI}(T)^2 = \text{tr}\,\mathbf{C}(T)\,\mathbf{C}(T)^{\dagger} = \sum_i^3 W_{D_i}(T)^2\, C_{D_i}(T)'^2 \sum_l^3 \rho_{il}(T)^2 \quad (24)$$

where I_{CI}(T) is the composite-index spectrum, † is the transpose, tr is the trace or the sum of the diagonal components and $\boldsymbol{\rho}(T)$ is a 3x3 period dependent matrix of correlation coefficients which were extracted from **Table 3** for period T=1.0 second, and its complete values covering all twenty-four periods were presented in **Table 9**. From the table, it could be

Diterima 8 Oktober 2021, Direvisi 31 Maret 2022, Diterima untuk dipublikasikan 25 April 2022

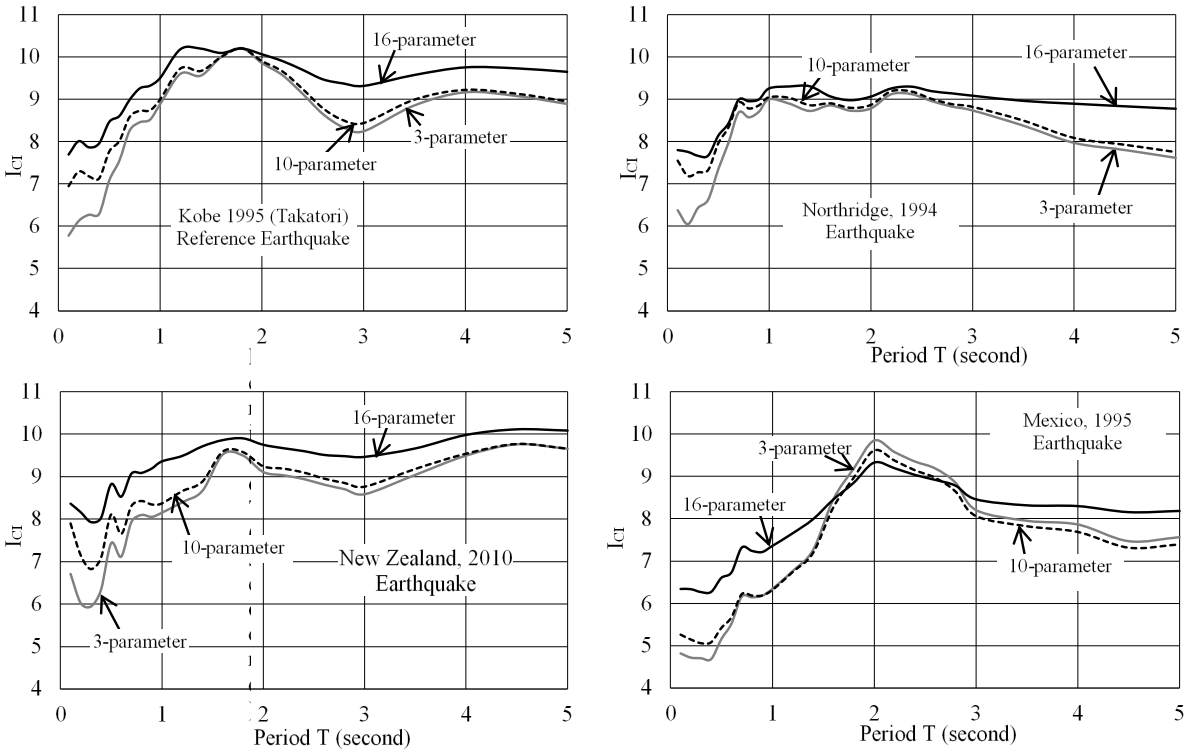

Figure 2. Composite-intensity index (I_{CI}) spectra for some earthquakes with 3-, 10-, and 16-parameters.

observed that Log $S_a(T)'$ was better correlated with Log PGV′ than with Log $D_{05\text{-}95}'$ for all periods; but it represented fewer parameters (see **Table 6**). It was also observable that the correlation coefficients among them as well as the weight factors were dependent on the periods. Further, it could be readily shown that $\sum_i^3 C_{Di}^{\,2} \le I_{CI}(T)^2 \le 3\sum_i^3 C_{Di}^{\,2}$ where the lower and upper bounds are associated with uncorrelated and fully correlated events, respectively.

The composite-index computed by **Eq. (24)** for the weighted normalized parameters were carried out 744 times covering all thirty-one earthquakes and twenty-four periods. The maximum value was 4.2964. It was scaled to an arbitrary number and was chosen to be 10.2 in the study, which indicated the highest composite-intensity index; the rests were scaled proportionally by a scale factor of 10.2/4.2964=2.3741. In this way each earthquake had its own composite-intensity index spectrum such as shown in **Figure 2** for some earthquakes. Kobe 1995 (Takatori) earthquake was the strongest among the thirty-one earthquakes investigated in this study so that it was set as the reference earthquake and given the maximum index of $I_{CI.max}$=10.2; followed by New Zealand 2010, and Northridge 1994. Mexico 1995 earthquake showed the most distinct character among the thirty-one earthquakes studied. It could be detrimental to a wide class of structures with periods less than 2 seconds especially when considering their effect of the period lengthening. The effect might stem from the inelastic behaviour of the structures and/or from the soil-structure interactions (Mylonakis and Syngros, 2004). Moreover, for such, considering only its PGA (0.21g) and PGV (71cm/sec) might be inadequate to properly characterize the earthquake (Goto and Morikawa, 2012), as they represented merely the highest and lowest frequencies as shown by Eqs. (8) and (9).

The earthquakes listed in **Table 1** were classified as strong motions as shown by their MMI scales of VII or higher. Meanwhile, the norm as computed by **Eq. (24)** was dependent on the value of κ in **Eq. (23)**. The value is so chosen that no parameter has negative values for all earthquake events after normalization (see Section 2 Point 6). To satisfy this condition, a minimum value of $I_{CI.min}$=3 was set in the study, and this corresponds to κ =3.5. Accordingly, among the low earthquakes in this scenario (numbers 7, 10, and 12 in **Table 1**), the lowest possessed the maximum $I_{CI.max}$=4.25 and the minimum $I_{CI.min}$=2.94 for earthquake number 7 (Imperial Valley 7, 1979, I_{MM}=VII).

To increase the confidence level, it is possible to include more parameters than the three discussed previously. Ten parameters from **Table 6** were then used to estimate about 80%, or about the mean-plus-sigma, of the composite-intensity index. Furthermore, if all sixteen parameters were included in the process, the confidence level would achieve the highest value in this study or about mean-plus-three sigma. The results for median, mean-plus-sigma and mean-plus-three sigma were shown in **Figure 2** for some earthquakes. It reflected the variabilities of the composite-intensity index from earthquake to earthquake and from frequency to frequency.

Diterima 8 Oktober 2021, Direvisi 31 Maret 2022, Diterima untuk dipublikasikan 25 April 2022

6. Relationship Between I_{MM} AND $I_{CI.MAX}$

To assess the structural damage potentials, the modified Mercalli intensity, I_{MM}, was employed in calibrating the composite-intensity index. The I_{MM} data in **Table 2** of all thirty-one earthquakes were plotted against the maximum values of the $I_{CI.max}$ for each earthquake. **Figure 3** presented such plots for 3-, 10- and 16-parameters. The linear regression relations of I_{MM} and $I_{CI.max}$ can be expressed as,

$$I_{MM} = m\, I_{CI.max} + n \quad (25)$$

where m=0.5933 and n=3.9371 (see **Figure 3**). From the three cases the slope and the intercept were set the same, and the standard error (S_{IMM}), as well as the coefficient of determination (R^2), were examined. They were of the same order, thus, showed good agreement among the three cases. Furthermore, by replacing $I_{CI.max}$ with $I_{CI}(T)$, **Eq. (25)** could be used to estimate the $I_{MM}(T)$ as dependent on the period, T, or the spectrum of I_{MM}, which was a new concept, albeit it was suggested long ago (Medvedev and Sponheuer, 1969).

7. Practical Application

The earthquake characterization procedure developed above was applied to practical application. For illustration when one acquired its own strong motion time series, then its composite-intensity index could be estimated by the following procedure. Suppose the earthquake strong motion was Chi-Chi earthquake, Taiwan, 1999, station TCU068, which was not in the data set (**Table 1**), downloaded from PEER (2020). Its acceleration spectrum, significant duration and peak ground velocity were presented in **Table 10**. For each parameter in the table, the mean and variance of the common logarithm parameters were computed as follows for Log PGV (and similarly for Log $S_a(T)$ and Log $D_{05\text{-}95}$),

$$\mu_{\text{Log } PGV} = \frac{1}{n}\left[\sum \text{Log } PGV\ (\text{Table 8}) + \text{Log } PGV(\text{Table 10})\right] \quad (26)$$

$$\sigma_{\text{Log } PGV}{}^2 = \frac{1}{n-1}\left[\sum [\text{Log } PGV]^2(\text{Table 8}) - n\left[\mu_{\text{Log } PGV}\right]^2\right] \quad (27)$$

where now n=32. The normalized Log PGV′ could then be computed by **Eq. (23)** as Log PGV′=(Log PGV $-\mu_{\text{Log PGV}}+3.5\ \sigma_{\text{Log PGV}})/\ \sigma_{\text{Log PGV}}$, and similarly for Log $S_a(T)$ and Log $D_{05\text{-}95}$. Multiply the normalized Log PGV′ by its weight factors indicated in **Table 9**; likewise, perform this step for Log $S_a(T)'$ and Log $D_{05\text{-}95}'$. Make use of **Eq. (24)** for the weighted parameters and coefficient of correlation $\rho(T)$ from **Table 9** to obtain the norm and multiply the resulting norm by the scale factor of 2.3741 (**Table 8**) to get the composite-intensity index spectrum, and then estimate the I_{MM} spectrum by **Eq. (25)**. The resulting I_{CI} and I_{MM} spectra were shown in **Figure 4** for 3-parameter; I_{MM} values were rounded to the closest integer. It could be observed that this earthquake was more damaging to the more flexible structures. Though, it could feel as I_{MM}=8 (T=0) for very short structures, for moderate high-rise structures it was perceived as 9 on the scale, and even 10 for taller structures. Moreover, the effect

Table 10. The acceleration spectrum, significant duration, and peak ground velocity of Chi-Chi earthquake (TCU068), Taiwan, 1999.

T s	S_a cm/s^2	T s	S_a cm/s^2	T s	S_a cm/s^2
0.10	996	1.00	1,014	2.80	687
0.20	949	1.20	995	3.00	642
0.30	1,330	1.40	895	3.50	551
0.40	1,501	1.60	843	4.00	565
0.50	1,438	1.80	869	4.50	605
0.60	1,121	2.00	787	5.00	668
0.70	932	2.20	723		
0.80	979	2.40	727	$D_{05\text{-}95}$ =	15.5 s
0.90	946	2.60	796	PGV =	311 cm/s

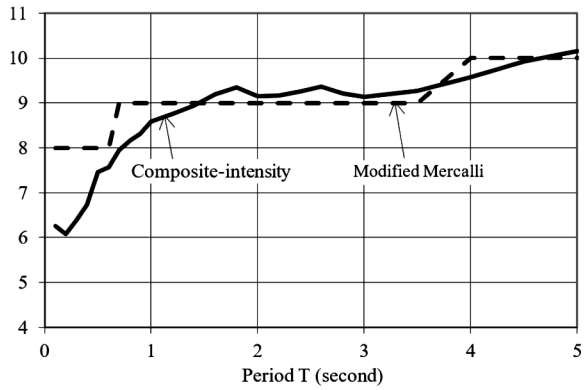

Figure 4. Composite-intensity index and I_{MM} spectra of Chi-Chi earthquake, Taiwan, 1999, station TCU068, 3-parameter

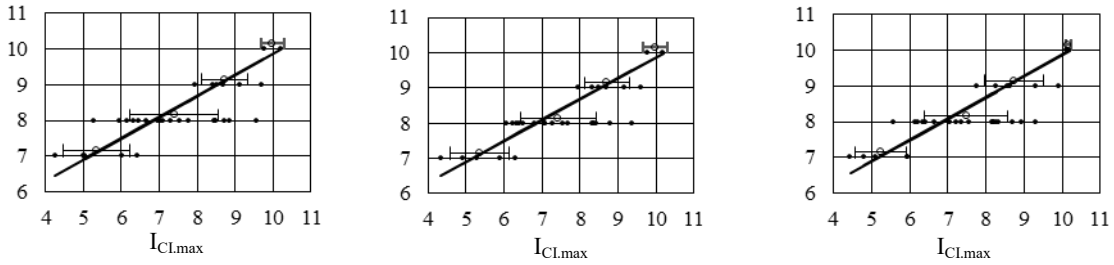

3-parameter; m=0.5933 n=3.9371; S_{IMM}=0.499 R^2=0.720

10-parameter; m=0.5933 n=3.9371; S_{IMM} =0.520 R^2=0.658

16-parameter; m=0.5933 n=3.9371; S_{IMM} =0.573 R^2=0.633

Figure 3. Plots between I_{MM} and $I_{CI.max}$ for 3-, 10-, and 16-parameters of the thirty-one earthquakes. Error bars of mean ± sigma and the regression relations of $I_{MM} = m\, I_{CI.max} + n$ are indicated

Diterima 8 Oktober 2021, Direvisi 31 Maret 2022, Diterima untuk dipublikasikan 25 April 2022

of period lengthening could increase the damage potential one scale-up for certain classes of structures. Structures with fundamental periods of, say, T=3.5 seconds, would experience periods lengthening due to inelastic deformation and the soil-structure interaction to become, say, 4 seconds. This corresponds with an increase of one MMI scale from 9 to 10 due to period lengthening phenomenon (Katsanos *et. al.* 2014). Such an increase in MMI scale could not be predicted by the currently available methodologies.

The study was performed based on the limited earthquake data set listed in **Table 1**. The accuracy of the results could be further improved by considering more data, or more specific events focusing on a certain region. This is also the case for the relation shown in **Figure 3** because the data in **Table 1** merely considered earthquakes with intensity $I_{MM} \geq 7$. However, the methodology developed herein is still applicable.

8. Conclusion

Based on the investigations outlined above, the following conclusions can be drawn:

1. An alternative method to strong earthquake ground motion characterization was formulated. The characterization was based on the spectral acceleration, $S_a(T)$, the significant duration, $D_{05\text{-}95}$, and the peak ground velocity, PGV. They were computed based on three-component earthquake ground motions. Each of these three parameters correlated to 80% or higher with other parameters it represented. Altogether, the three parameters represented nine to ten other parameters of sixteen totally, or about 63%, resulting in a median value confidence level. The three parameters were combined to yield the composite-intensity index.
2. The index, I_{CI}, was related to the modified Mercalli intensity, I_{MM}, to assign its damage potentials. Thirty-one three-component earthquake records collected worldwide were studied. Among these earthquakes, the well-known Kobe 1995 (Takatori), New Zealand 2010, and Northridge 1994 were among the strongest earthquakes. The Mexico 1995 earthquake showed the most distinct character which could be more detrimental when considering the period elongation of structures.
3. Practical application to Chi-chi earthquake showed more meaningful interpretations of its characters. The damage potentials of Chi-chi showed that at a lower period than about 0.8 seconds it was perceived as 8 MMI; but it was 10 MMI for periods higher than 4 seconds; and 9 MMI in between them. It became critical at the transition periods as the period elongation due to inelastic response and soil-structure interaction might be an issue.

Acknowledgement

The authors acknowledged the support of the Engineering Centre for Industry and the Centre for Infrastructures and Built Environment, both of Institute of Technology Bandung. The authors also gratefully acknowledged the constructive comments by the anonymous reviewer.

References

Ang, A. H. S. and Tang, W. H. (2007) "Probability concepts in engineering: Emphasis on applications in civil and environmental engineering," John Wiley & Sons.

Arias A. (1970) "A measure of earthquake intensity," in Seismic Design for Nuclear Power Plants, ed. R. J. Hansen (MIT Press, Cambridge, MA), 438–483.

Baker, J.W. and Cornell, C.A. (2006) "Which Spectral Acceleration Are You Using?," Earthq. Spectra, 22, 293-312.

Bijukchhen, S., Takai, N., Shigefuji, M., Ichiyanagi, M. and Tsutomu, S.T. (2017) "Strong-Motion Characteristics and Visual Damage Assessment around Seismic Stations in Kathmandu after the 2015 Gorkha, Nepal, Earthquake," Earthq. Spectra, 33(S1), S219-S242.

Bommer, J.J. and Martínez-Pereira, A., (1999) "The Effective Duration of Earthquake Strong Motion," J. Earthq. Eng., 3(2), 127-172.

Bommer, J.J. and Alarcon, J.E. (2006) "The Prediction and Use of Peak Ground Velocity," J. Earthq. Eng., 10, 1-31.

Bozorgnia, Y. and Campbell, K.W. (2004) "Engineering Characterization of Ground Motion," in Earthquake Engineering: From Engineering Seismology to Performance-Based Engineering, Bozorgnia, Y. and Bertero, V.V., Chapter 5, 215-315.

Bradley, B.A. (2012) "Empirical Correlations between Peak Ground Velocity and Spectrum-Based Intensity Measures," Earthq. Spectra, 28, 17-35.

Campbell, K.W. and Bozorgnia, Y. (2012) "Cumulative Absolute Velocity (CAV) and Seismic Intensity Based on the PEER-NGA Database," Earthq. Spectra, 28(2), 457-485.

Elenas, A. (2000) "Correlation between Seismic Acceleration Parameters and Overall Structural Damage Indices of Building," Soil Dynam Earthquake Eng., 20, 93-100.

Fajfar, P., Vidic, T. and Fischinger, M. (1990) "A measure of earthquake motion capacity to damage medium-period structures," Soil Dynam Earthquake Eng.,9(5), 236-242.

Garcia, A.G. and Bernal, A.G. (2008) "Relationships between Instrumental Ground Motion Parameters and the Modified Mercalli Intensity in Guerrero, Mexico," 14th World Conference on Earthquake Engineering, Beijing, China.

Diterima 8 Oktober 2021, Direvisi 31 Maret 2022, Diterima untuk dipublikasikan 25 April 2022

Ghobarah, A. and Elnashai, A.S. (1998), "Contribution of vertical ground motion to the damage of R/C buildings," Proceedings of the 11th European Conference on Earthquake Engineering, Balkema, 468-477.

Goto, H. and Morikawa, H. (2012) "Ground motion characteristics during the 2011 off the Pacific Coast of Tohoku Earthquake," Soil Mech Found Eng., 52(5), 769-779.

Hancock, J. and Bommer, J.J. (2006) "A State-of-Knowledge Review of the Influence of Strong-Motion Duration on Structural Damage," Earthquake Spectra, 22(3), 827-845.

Housner, G.W. (1952) "Spectrum intensities of strong-motion earthquakes," Symposium on Earthquakes and Blast Effects on Structures, Los Angeles, CA.

Katsanos, E.I., Sextos, A.G. and Elnashai, A.S. (2014) "Prediction of inelastic response periods of buildings based on intensity measures and analytical model parameters," Eng Struct. , 71, 161-177.

Luco, N. and Cornell, C. (2007), "Structure-Specific Scalar Intensity Measures for Near-Source and Ordinary Earthquake Ground Motions," Earthq. Spectra, **23**(2), 357-392.

Massumi, A. and Selkisari, M.R. (2017) "Correlations between Spectral Parameters of Earthquakes and Damage Intensity in Different RC Frames," Eng Geol., 11(3), 133-158.

Medvedev, S.V. and Sponheuer, W. (1969) "Scale of Seismic Intensity," 4th World Conference Earthquake Engineering, Santiago, Chile, A-2, 143-153.

Mylonakis, G. and Syngros, C. (2004), "The Collapse of Fukae (Hanshin Expressway) Bridge, Kobe, 1995: The Role of Soil and Soil-Structure Interaction," International Conference on Case Histories in Geotechnical Engineering, 12.

PEER (2020) "Ground Motion Database," Pacific Earthquake Engineering Research Center.

Perrault, M. and Guéguen, P. (2015), "Correlation between Ground Motion and Building Response Using California Earthquake Records," Earthq. Spectra, 31(4), 2027-2046.

Sandeep, G.S. and Prasad, S.K. (2012) "Housner Intensity and Specific Energy Density for Earthquake Damage Assessment from Seismogram," Proceedings of International Conference on Advances in Architecture and Civil Engineering, Karnataka, India.

Trifunac, M.D. and Brady, A.G. (1975) "A Study on Duration of Strong Earthquake Ground Motion," Bulletin of the Seismological Society of America, 65, 581-626.

Von Thun, J., Roehm, L., Scott, G., Wilson, J. (1988) "Earthquake Ground Motions for Design and Analysis of Dams", Earthquake Engineering and Soil Dynamics II-Recent Advances in Ground-Motion Evaluation, Geotechnical Special Publication, 463-481.

Wald, D. J., Quitoriano, V., Heaton, T. H. and Kanamori, H. (1999) "Relationships between peak ground acceleration, peak ground velocity, and Modified Mercalli Intensity in California," Earthq. Spectra, 15, 557–564.

Wood, H.O. and Neumann, F. (1931) "Modified Mercalli Intensity Scale of 1931," Bull Seismol Soc Am., 21(4), 277-283.

Wu, H., Masaki, K., Irikura, K., Saguchi, K., Kurahashi, S. and Wang, X. (2012) "Relationship between Building Damage Ratios and Ground Motion Characteristics during the 2011 Tohoku Earthquake," J. Natural Disaster Science, 34(1), 59-78.

Wu, Y.M., Teng, T.L., Shin, T.C. and Hsiao, N.C. (2003) "Relationship between Peak Ground Acceleration, Peak Ground Velocity, and Intensity in Taiwan," Bull Seismol Soc Am., 93, 386-396.

Xie, J., Wen, Z. and Li, X. (2012), "Characteristics of Strong Motion Duration from the Wenchuan M_w 7.9 Earthquake," 15th World Conference on Earthquake Engineering, Lisboa.

Zhang, Y., He, Z. and Yang, Y. (2018) "A Spectral-Acceleration-Based Linear Combination-Type Earthquake Intensity Measure for High-Rise Buildings," J. Earthq. Eng., 22(8), 1479-1508.

Diterima 8 Oktober 2021, Direvisi 31 Maret 2022, Diterima untuk dipublikasikan 25 April 2022